Rifts in Rafts

Khá-Î Tô[1] and Sidney R. Nagel[1]

[1]The Department of Physics and the James Franck and Enrico Fermi Institutes
The University of Chicago IL 60637.

This PDF contains:

- Supplementary Information Text
- Fig. S1
- Fig. S2
- Legends for Movies S1 to S6

Derivation of Eq. 4

We start from Eq. 3 and write down the terms inside the modified Bessel's function K_1 explicitly:

$$3\pi\eta d\alpha\frac{du(x_j)}{dt} = \pi\sigma d B^{5/2}\Sigma^2\Big(- K_1(\frac{\Delta x + u(x_j) - u(x_{j-1})}{L_c}) + K_1(\Delta x + \frac{u(x_{j+1}) - u(x_j)}{L_c})\Big)$$

After using the asymptotic form of $K_1(x) \approx 1/x$ when $x \ll 1$, we obtain:

$$\begin{aligned}\frac{du(x_j)}{dt} &\approx \frac{\sigma B^{5/2}\Sigma^2}{3\pi\eta\alpha}\Big(- \frac{1}{\Delta x + u(x_j) - u(x_{j-1})} + \frac{1}{\Delta x + u(x_{j+1}) - u(x_j)}\Big)\\ &\approx \frac{\sigma B^{5/2}\Sigma^2}{3\pi\eta\alpha}\frac{1}{\Delta x}\Big(- \frac{1}{1 + \frac{u(x_j)-u(x_{j-1})}{\Delta x}} + \frac{1}{1 + \frac{u(x_{j+1})-u(x_j)}{\Delta x}}\Big)\end{aligned}$$

Since $u(x)$ is a small perturbation, we can then Taylor expand to the first order of $u(x)$:

$$\begin{aligned}\frac{du(x_j)}{dt} &\approx \frac{\sigma B^{5/2}\Sigma^2}{3\pi\eta\alpha}\frac{1}{\Delta x}\Big(- 1 + \frac{u(x_j) - u(x_{j-1})}{\Delta x} + 1 + \frac{u(x_{j+1}) - u(x_j)}{\Delta x}\Big)\\ &\approx -\frac{\sigma B^{5/2}\Sigma^2}{3\pi\eta\alpha}\frac{1}{\Delta x^2}\Big(u(x_{j+1}) + u(x_{j-1}) - 2u(x_j)\Big)\end{aligned}$$

After taking this equation to the continuum limit, we obtain:

$$\frac{\partial u}{\partial t} = -(\frac{\sigma B_o^{5/2}\Sigma^2 L_c}{3\eta\alpha})\frac{\partial^2 u}{\partial x^2}$$

Results of pair-correlation

We use a high-resolution camera to film the particles in the raft. We extract the centroid of each particle and from those positions calculate the pair-correlation function, $g(x, y)$, and the structure factor, $S(k_x, k_y)$. We compare the results before the raft is stretched, $\varepsilon = 0.0$, with the results after the raft has been stretched to $\varepsilon = 1.0$. In Fig. S1A, we show $g(x, y)$ for a particle raft, with initial dimensions $L_{x0} \approx 37\ mm$ and $L_{y0} \approx 65\ mm$ floating on a distilled water surface pulled in the x-direction at speed $V = 12\ mm/s$. For this situation, $\langle\ell\rangle \approx 6d$. The results in Fig. S1A show that the particles are distributed isotropically for $\varepsilon = 0.0$. However, even when $\varepsilon = 1.0$, it is difficult to see a

strong variation between the x- and y-directions. The structure becomes more blurred out after a few rings. There is clearly less correlation, but it is difficult to see an obvious signal of cluster and rift formation. In Fig. S1B, we show the results for $S(k_x, k_y)$ using the same set of data. This data, too, does not produce a strong signature of the cluster or rift structures.

Effects of secondary flows

Localized features in the rafts

In Fig. 2A and the movies, we observe some features in the rafts in addition to the homogeneous length structures we focus in the main text at different velocity regimes and boundary conditions. They are introduced by the secondary flows, that is the non-affine components in the expansion metric. For the highest strain rate, in both repulsive (right column of Fig. 2A and movie S3) and attractive boundaries (movie S6), we see the influence of surface waves in the third dimension due to the high pulling speeds. The accumulation of particles next to the pullers is due to the formation of a trough near those boundaries. This is more prominent if we go even faster. For low-speed experiments, we observe different behaviors for different boundary conditions. For the attractive boundary (movie S1), the raft fractures into pieces caused by the localized eddy currents generated at the slits between the pullers and the sidewalls. Once an initial notch is formed at the weakest point, the liquid will keep flowing into this newly-created space and shear the raft. There is also extra forces between the raft and the pullers. As the center of the raft remains still, the raft is forced to break apart. For repulsive boundary conditions (left column of Fig. 2A and movie S1), since the raft is not attached to the pullers, it can remain intact. Therefore, as the pullers move, the secondary flows only go into the tiny space between the raft and the pullers.

Comparison between attractive and repulsive boundary conditions

In Fig. S2, we show the results from air-water experiments with both attractive and repulsive boundary conditions. The results are shown at a slightly smaller strain ($\varepsilon = 0.7$) than the one in the main text because the rafts in the low-speed experiments with attractive boundary conditions break apart quickly. The average cluster length, $\langle \ell \rangle$, measured in both boundary conditions are very similar from intermediate to high pulling speed V. Because the rafts are attached to the pullers, they are forced to break into pieces when the pullers are sufficiently separated. Therefore, the data points from the attractive boundary condition level off to a constant value at low V. This leads to a much smaller dynamic range for the measurements with attractive boundary conditions.

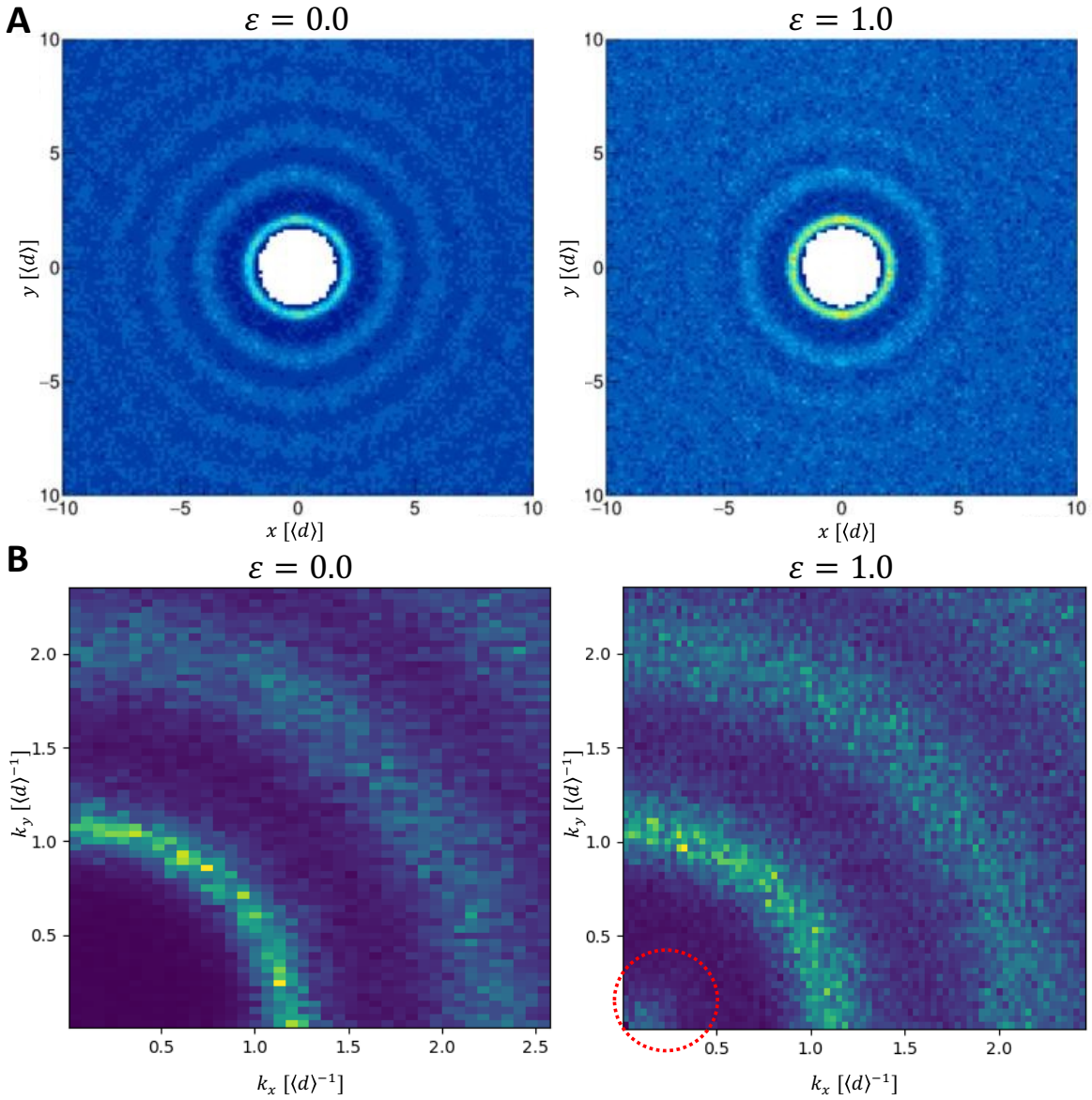

Figure 1: Pair-correlation function and structure factor. (A) The pair-correlation function, $g(x, y)$ for a raft (left) before being stretched $\varepsilon = 0.0$ compared to the result (right) after the raft has been stretched to $\varepsilon = 1.0$. (B) The structure factor $S(k_x, k_y)$ computed from the same data as in (A). Left: $\varepsilon = 0.0$. Right: $\varepsilon = 1.0$. After having been stretched, there is a weak signature at $|\mathbf{k}| < 1$ (shown in the dashed red circle), which corresponds to the appearance of a length scale larger than the average particle diameter.

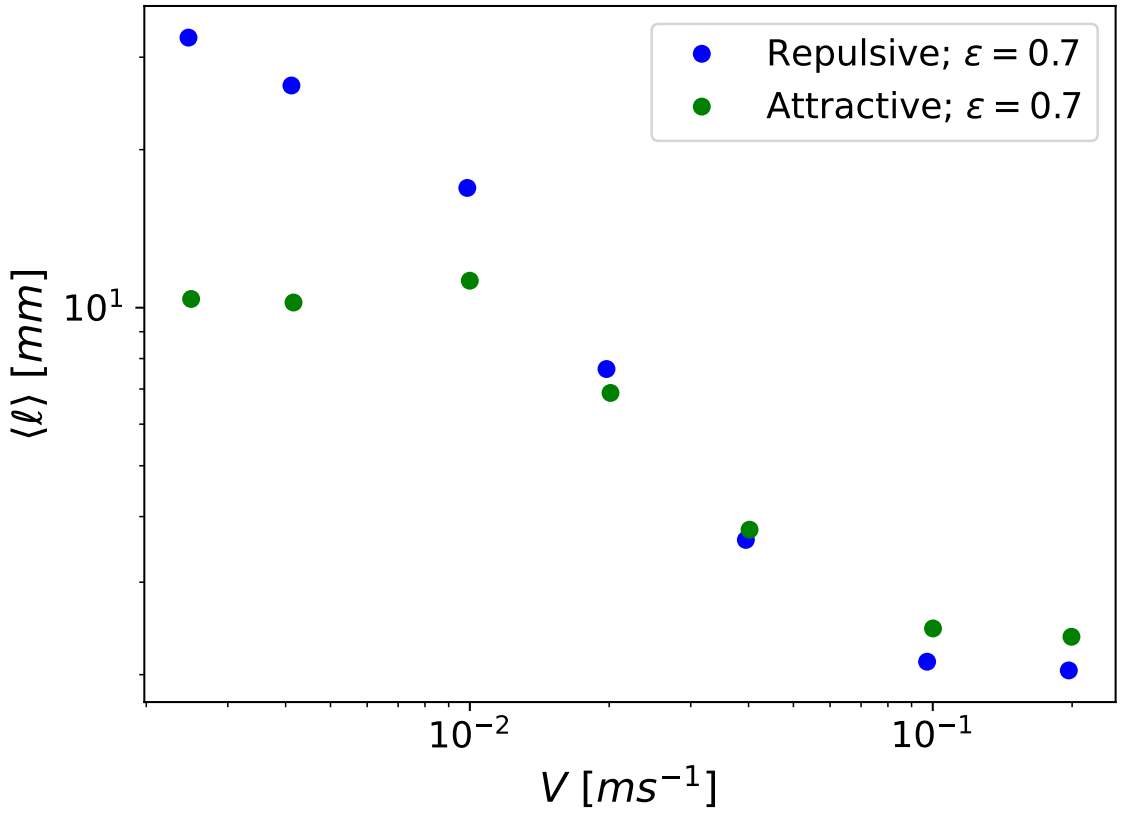

Figure 2: Average cluster length, $\langle \ell \rangle$, vs. pulling speed, V, at fixed strain $\varepsilon = 0.7$ for both attractive and repulsive boundary conditions.

Movie S1. Air-water experiment with repulsive boundaries for pulling speed $V = 2.5\ mm/s$. (Sped up by 15×.)
Movie S2. Air-water experiment with repulsive boundaries for pulling speed $V = 20\ mm/s$. (Sped up by 2×.)
Movie S3. Air-water experiment with repulsive boundaries for pulling speed $V = 200\ mm/s$. (Slowed down by 5×.)
Movie S4. Air-water experiment with attractive boundaries for pulling speed $V = 2.5\ mm/s$. (Sped up by 15×.)
Movie S5. Air-water experiment with attractive boundaries for pulling speed $V = 20\ mm/s$. (Sped up by 2×.)
Movie S6. Air-water experiment with attractive boundaries for pulling speed $V = 200\ mm/s$. (Slowed down by 5×.)